Diffusion, aggregation, and the thermal conductivity of nanofluids

Patricia E. Gharagozloo,[a] John K. Eaton, and Kenneth E. Goodson
Stanford University, Building 530, 440 Escondido Mall, Stanford, California 94305, USA

(Received 31 July 2008; accepted 14 August 2008; published online 11 September 2008)

The effects of nanoparticle aggregation and diffusion are difficult to separate using most nanofluid thermal conductivity data, for which the temperature dependence is collected sequentially. The present work captures the instantaneous temperature-dependent thermal conductivity using cross-sectional infrared microscopy and tracks the effects of aggregation and diffusion over time. The resulting data are strongly influenced by spatial and temperature variations in particle size and concentration and are interpreted using a Monte Carlo simulation and rate equations for particle and heat transport. These experiments improve our understanding of nanofluid behavior in practical systems including microscale heat exchangers. © *2008 American Institute of Physics*.
[DOI: 10.1063/1.2977868]

The last decade has brought some progress in our understanding of thermal conduction by nanofluids, nanoscale particles suspended in liquids. One motivation has been the need for fluids with higher thermal conductivities in fluidic cooling systems for applications including microprocessors and high-power lasers. Improvements in fluid conductivity have varied strongly with synthesis method and particle type, size, and concentration. Data are compared using $\alpha_k \equiv (k_{\text{eff}}/k_f - 1)/\varphi$, with effective thermal conductivity k_{eff}, base fluid thermal conductivity k_f, and particle volume fraction φ. In water and organic compounds, α_k data vary from 1.5 to 30 and 6 to 10 with oxide particles, respectively, from 30 to 240 and 10 to 65 with metal particles, and from 20 to 120 in both with carbon nanotubes.[1–16] Much of the research found thermal conductivity enhancements greater than predictions by effective medium theory (EMT), at low volume concentrations, yielding many proposed models.[17–29]

Several groups have studied conductivity time evolution. Hong *et al.*[7] measured a 0.2% volume concentration of 10 nm Fe particles in ethylene glycol and found the actual particle size to increase from 1.2 to 2.3 μm and the enhancement to decrease from 14% to 9% after 1 h. Karthikeyan *et al.*[15] measured 0.8% and 0.3% volume concentrations of 8 nm CuO particles in water and found enhancements of 23% and 17%, respectively, decreased to 0% after 20 min. Actual particle sizes were not reported. A 1% volume concentration of 40 nm Al_2O_3 particles in water with initial particle size of 160 nm, captured with dynamic light scattering (DLS), yielded a 3% conductivity decrease over 12 min.[16]

Aggregation and thermodiffusion both change thermal conductivity with time. Predictions[28–31] indicate an increase in conductivity with aggregation in contrast with recent data.[7,15,16] Calculations by Prasher *et al.*[28,29] Keblinski *et al.*,[30] and Eastman *et al.*[31] give potential α_k values up to 10 rather than the value of 3 given by EMT. Large conductivity increases with aggregation are possible in stable nanofluids. However, in unstable nanofluids particles become large and settle, decreasing concentration and thermal conductivity. A nanofluid with sufficient stability to enable a temporal increase in conductivity has yet to be reported.

While the direct contribution of thermodiffusion to heat conduction is negligible,[16,22] particle diffusion strongly influences the local concentration and conductivity.[16–19] Buongiorno[17] and Wen and Ding[19] found with particle diffusion models in flow that particle migration results in significant particle concentration nonuniformities altering conductivity profiles. Savino and Paterna[18] showed in horizontal cavity models that the combined gradients in concentration and temperature produce circulation. Thermodiffusion effects on nanofluid properties have yet to be examined experimentally. However, thermodiffusion influences particle distributions in many conductivity measurement techniques. The hotwire technique applies a temperature gradient inducing heat flux. Particle diffusion away from the hotwire could yield lower concentration and thus lower conductivity measurements. The thermodiffusion effects increase in radial systems with a centered heat source and larger colder volume.

Until now, measurements of the thermal properties of nanofluids could not separate the transient effects. Past measurements were taken successively over time while varying one property, such as temperature, without accounting for other effects, such as thermodiffusion and aggregation. The joint effects of these cause interdependencies where the aggregation time constant decreases with temperature and concentration and diffusion decreases with aggregate size. A technique for instantaneous measurements of the full field thermal properties of the nanofluid is needed.

This letter presents measurements of both the temporal and spatial variations of the thermal conductivity of nanofluids subjected to a temperature gradient. The resulting data capture changes in thermal conductivity across the temperature gradient over time and provide a unique chance to separate the effects of aggregation and thermodiffusion. The full field temperature distribution is measured with a high-resolution infrared microscope (QFI/Infrascope). Figure 1 shows a schematic of the experimental setup. 1 in. square, copper plates spaced 500 μm apart hold the nanofluid. This spacing yields an average Rayleigh number less than 10^3 and scaling analysis confirms that bulk fluidic motion due to buoyancy forces is negligible. The IR focal plane array is 256×256 InSb with 2–5.5 μm wavelength detection and 0.1 K temperature sensitivity. A 15×, 1.0 numerical aperture,

[a]Electronic mail: p.gharagozloo@stanford.edu.

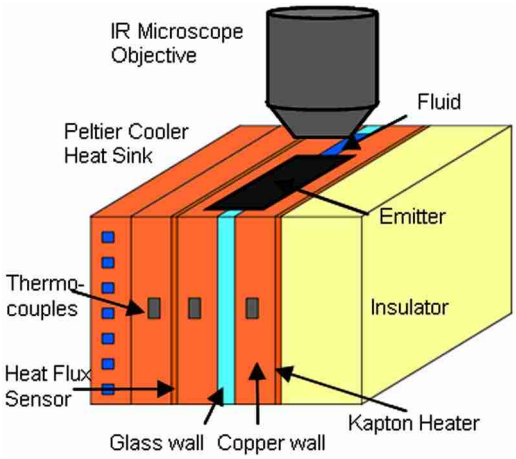

FIG. 1. (Color online) Schematic of IR microscope experimental setup with nanofluid held between copper plates. A heat flux is applied across the nanofluid with a thin Kapton heater, measured on the opposite side with a heat flux sensor, and dissipated into a Peltier cooler and heat sink. The temperature is monitored with thermocouples on the copper plates.

Si/Ge objective obtains a 2.8 μm resolution. The 256 temperature lines are ensemble averaged. A 250 μm thick Kapton heater (Omega/KHLV-101) generates Joule heat, which conducts across the nanofluid, and dissipates into a Peltier cooler and heat sink. A heat flux sensor (Omega/HFS-3) monitors the heat flux. An encasing humidification chamber reduces evaporation. A 20 μm thick polyester film covers the fluidic opening, serves as a uniform emissivity emitter, counteracts averaging effects from the IR penetration in water, and reduces fluid evaporation. The heat flux traveling through the film is calculated using a thermal resistor network as less than 0.06% of the applied heat flux. A COMSOL finite element model thermal predicts the difference in the calculated thermal conductivity from the temperature of the film compared to the fluid temperature of less than 1%. The emissivity is calibrated for each measurement with a two temperature surface emissivity correction at characteristic temperatures. The calibration is applied to the measurement images and corrects for reflected signal components and emissivity spatial and temperature dependencies.

Heat loss from the experimental apparatus to the environment is due to natural convection from the outer surfaces, conduction through the back insulator, and fluid evaporation. These losses are found to be less than 5% of the applied heating power and are systematically eliminated as part of the data extraction procedure. The ability to precisely determine the temperature-dependent conductivity of pure water is verified before each measurement. The thermal conductivities have repeatability to within 5% of the average value.

The nanofluid is purchased with 20% by weight alumina in H_2O with less than 1% nitric acid (Alfa Aesar/ 12733). The fluid is diluted with deionized water to the desired concentrations. Prior to the measurements the nanofluid is sonicated for 4 h. The nanofluid is stable with only minor settling after a week. DLS measurements performed on a solution diluted to 0.5% by volume yield a nominal particle size of 90 nm and polydispersity of 0.244.

A set of rate equations are evaluated to model the combined effects of temperature and concentration gradients on particle and heat diffusion:[32]

$$q'' = -c_1 \nabla n - c_2 \nabla T, \tag{1}$$

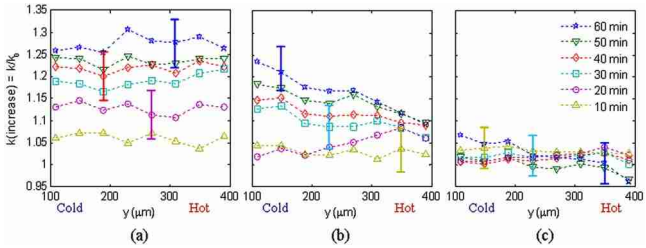

FIG. 2. (Color online) Time dependence of the full field thermal conductivity increase of a nanofluid consisting of alumina particles in water in a temperature gradient for volumetric concentrations of (a) 5%, (b) 3%, and (c) 1%. While the experimental uncertainty makes it impossible to extract conclusions for the case of 1% concentration, the trends observed for the other two concentrations are significant beyond the uncertainty.

$$j = -D \nabla n - nD_T \nabla T, \tag{2}$$

with particle flux j, particle number density n, diffusion coefficient D, thermal diffusivity D_T, heat flux q'', temperature T, and unknown constants c_1 and c_2. At steady state, zero particle flux gives the Soret equation

$$0 = -\nabla n - nS_T \nabla T \tag{3}$$

with the Soret coefficient $S_T \equiv D_T/D$. Removing the dependence of ∇n in Eq. (1) using Eq. (3) yields

$$q'' = (c_1 nS_T - c_2) \nabla T \tag{4}$$

yielding $-(c_1 nS_T - c_2)$ as the apparent fluid thermal conductivity. Combining Eqs. (1) and (2) in the yields

$$q'' = c_1 j/D - (c_2 - c_1 nS_T) \nabla T, \tag{5}$$

where the first term is heat flux due to particle flux and is approximated by heat flux due to mass flux, $\dot{m}/A$ below

$$q''_{\text{particle flux}} = (\dot{m}/A) c_p \Delta T \approx j m_p c_p \Delta T \tag{6}$$

with mass flux approximated by the product of particle flux at uniform concentration, channel area, and particle mass. Using experimentally representative values, we find the upper limit to heat flux due to particle flux is of order 10^{-2} W/m^2, c_1 is of order 10^{-25} W m^2/particle, and $(c_1 nS_T)$ is of order 10^{-7} W/m K, which is much smaller than the fluid thermal conductivity. Additionally, $c_1 \nabla n$ is on the order of 10^{-2} W/m^2 which is much smaller than $c_2 \nabla T$ on the order of 10^4 W/m^2 leaving Fourier's law for heat diffusion,

$$q'' = -k_{\text{eff}} \nabla T. \tag{7}$$

Equation (7) calculates the effective conductivity from the measured temperature gradient and heat flux. The total temperature difference across the gap is about 25 °C with 25 W of heating and a mean temperature of 50 °C. Emitter film curvature at the edge of the copper plates prevents evaluation of the outer 70 μm of the image. The conductivity profile is evaluated by calculating the slope of nine 40 μm temperature divisions with 50% overlap. Figure 2 plots the increase in the measured nanofluid conductivity over time for 5%, 3%, and 1% volume concentrations. Small droplets condensing on the emitting film during the measurement create slight waviness in the plots which slightly skew the calculations.

The 1% volume concentration yields no discernable changes in conductivity over time considering the experimental uncertainty. The 5% volume concentration yields a 30% increase in thermal conductivity over time across the

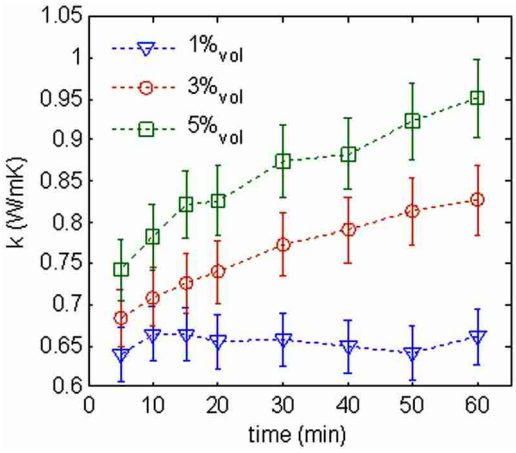

FIG. 3. (Color online) Time dependence of average thermal conductivity for varying concentration in nanofluid consisting alumina particles in water.

entire sample. The 3% volume concentration yields an increase in thermal conductivity over time with a larger increase on the cold side of the fluid. Diffusion toward the cold side increases the local concentration, allowing greater thermal conductivity increase from clustering. Particle diffusion away from the hot side decreases the concentration, limiting conductivity increase. Prasher *et al.*[28] shows the increase in conductivity is greater for higher concentrations at the same aggregate radius, and that the aggregation time constant is inversely proportional to concentration yielding faster aggregation at higher concentrations. Their calculations show possible enhancements, with an aggregate radii ten times the particle radii, of 5% for 1% volume concentration, 12% for 2% volume concentration, and 30% for 4% volume concentration. Higher concentrations yield much faster and larger enhancements.

To interpret the experimental data, a two-dimensional Monte Carlo simulation based on Brownian diffusion estimates the concentration variation and Soret coefficient of the sample. The simulation uses 250 000 particles with sizes distributed according to DLS measurements. The particles are initially uniformly distributed and a temperature gradient is applied as in the experiments. At each time step, a normally distributed random kick is applied to each particle in the x and y directions with mean zero and variance $2D\Delta t$. The simulation accounts for the viscosity and diffusion coefficient temperature dependence and for diffuse reflection at fluid boundaries. The resulting estimate for the effective Soret coefficient in the fluids examined here, 0.02 K^{-1}, compares to estimated values ranging from 0.01 to 0.1 K^{-1} for C_{60}-C_{70} fullerenes and 4 nm gold particles.[11] The predicted concentration variation for the 3% nanofluid after 1h is from 4% to 2.5% from the cold to hot side. The faster aggregation in the 5% volume concentration could reduce thermodiffusion and uniform clustering may create the uniform increase in thermal conductivity. At higher temperatures, Prasher *et al.*[28] predict smaller aggregation time constants, which could balance thermodiffusion effects.

Figure 3 plots the time dependence of the average conductivity. We observe large temporal increases in thermal conductivity for 3% and 5% concentrations and none for 1% concentration. These data are consistent with the previously mentioned models[28–31] with upper α_k values of 10.

In summary, the full field temperature distribution allows the extraction of information not obtained using other measurement techniques. Aggregation in stable nanofluids significantly increases the thermal conductivity of the fluid. Thermodiffusion affects the amount of aggregation across a temperature gradient by imposing a concentration distribution and variation in the aggregation time constant. The thermal conductivity distribution is affected through its direct relationship with the concentration and progress of aggregation. Future studies of aggregate progression and thermodiffusion through light scattering techniques are needed to understand how the aggregation and concentration vary over time in the temperature gradient.

The authors acknowledge the financial support from the Office of Naval Research through Contract No. N00014-05-0374-P00001 and graduate fellowships from the National Science Foundation and Sandia National Laboratories. The authors thank Babajide Kolade and Joo-Hyun Lee for their technical collaboration on nanofluids and measurements.

[1] S. Kabelac and J. F. Kuhnke, IHTC Keynote, 2006 (unpublished), Paper No. 10.1615/IHTC13, p. 30.
[2] J. A. Eastman, S. U. S. Choi, S. Li, W. Yu, and L. J. Thompson, Appl. Phys. Lett. **78**, 718 (2001).
[3] S. Murshed, K. Leong, and C. Yang, Int. J. Therm. Sci. **44**, 367 (2005).
[4] M. Liu, M. Lin, C. Tsai, and C. Wang, Int. J. Heat Mass Transfer **49**, 3028 (2006).
[5] X. Zhang, H. Gu, and M. Fujiji, Int. J. Thermophys. **27**, 569 (2006).
[6] Y. Xuan and Q. Li, Int. J. Heat Fluid Flow **21**, 58 (2000).
[7] K. Hong, T. Hong, and H. Yang, Appl. Phys. Lett. **88**, 031901 (2006).
[8] T. K. Hong, H. S. Yang, and C. J. Choi, J. Appl. Phys. **97**, 064311 (2005).
[9] S. Das, N. Putra, P. Thiesen, and W. Roetzel, J. Heat Transfer **125**, 567 (2003).
[10] H. Xie, J. Wang, T. Xi, Y. Liu, F. Ai, and Q. Wu, J. Appl. Phys. **91**, 4568 (2002).
[11] S. A. Putnam, D. G. Cahill, P. V. Braun, Z. Ge, and R. G. Shimmin, J. Appl. Phys. **99**, 084308 (2006).
[12] C. H. Li and G. P. Peterson, J. Appl. Phys. **99**, 084314 (2006).
[13] J. Eastman, S. Choi, S. Li, L. Thompson, and S. Lee, MRS Symposia Proceedings (Materials Research Society, Pittsburgh, 1997), Vol. 457, p. 3.
[14] M. Chopkar, P. K. Das, and I. Manna, Scr. Mater. **55**, 549 (2006).
[15] N. R. Karthikeyan, J. Philip, and B. Raj, Mater. Chem. Phys. **109**, 50 (2008).
[16] P.E. Gharagozloo, K.E. Goodson, J.K. Eaton, ASME InterPACK, Vancouver, BC, 33293, 2007.
[17] J. Buongiorno, J. Heat Transfer **128**, 240 (2006).
[18] R. Savino and D. Paterna, Phys. Fluids **20**, 017101 (2008).
[19] D. Wen and Y. Ding, Microfluid. Nanofluid. **1**, 183 (2005).
[20] R. Prasher, P. Bhattacharya, and P. Phelan, Phys. Rev. Lett. **94**, 025901 (2005).
[21] W. Evans, J. Fish, and P. Keblinski, Appl. Phys. Lett. **88**, 093116 (2006).
[22] Q. Z. Xue, Phys. Lett. A **307**, 313 (2003).
[23] J. Koo and C. Kleinsteuer, Int. Commun. Heat Mass Transfer **32**, 1111 (2005).
[24] Y. Ren, H. Xie, and A. Cai, J. Phys. D **38**, 3958 (2005).
[25] B. Wang, L. Zhou, and X. Peng, Int. J. Heat Mass Transfer **46**, 2665 (2003).
[26] P. Bhattacharya, S. K. Saha, A. Yadav, P. E. Phelan, and R. S. Prasher, J. Appl. Phys. **95**, 6492 (2004).
[27] J. Eapen, J. Li, and S. Yip, Phys. Rev. E **76**, 062501 (2007).
[28] R. Prasher, W. Evans, P. Meakin, J. Fish, P. Phelan, and P. Keblinski, Appl. Phys. Lett. **89**, 143119 (2006).
[29] R. Prasher, P. Phelan, and P. Bhattacharya, Nano Lett. **6**, 1529 (2006).
[30] P. Keblinski, J. A. Eastman, and D. G. Cahill, Mater. Today **8**, 36 (2005).
[31] J. A. Eastman, S. R. Phillpot, S. U. S. Choi, and P. Keblinski, Annu. Rev. Mater. Res. **34**, 219 (2004).
[32] D. E. Winterbone, *Advanced Thermodynamics for Engineers* (Wiley, New York, 1997).